Inderpreet Kaur; Andrea Mentrelli; Frederic Bosseur; Jean Baptiste Filippi; Gianni Pagnini

Wildland fire propagation modelling: A novel approach reconciling models based on moving interface methods and on reaction-diffusion equations

Persistent URL: http://dml.cz/dmlcz/702967

WILDLAND FIRE PROPAGATION MODELLING: A NOVEL APPROACH RECONCILING MODELS BASED ON MOVING INTERFACE METHODS AND ON REACTION-DIFFUSION EQUATIONS

Inderpreet Kaur[1], Andrea Mentrelli[1,2], Frederic Bosseur[3],
Jean Baptiste Filippi[3], Gianni Pagnini[1,4]

[1] BCAM - Basque Center for Applied Mathematics
Alameda de Mazarredo 14, 48009 Bilbao, Basque Country – Spain
ikaur@bcamath.org
[2] Department of Mathematics and AM^2, University of Bologna
Via Saragozza 8, 40123 Bologna, Italy
andrea.mentrelli@unibo.it
[3] SPE–CNRS/University of Corsica, Corte, Corsica – France
fbosseur@gmail.com; filippi@univ-corse.fr
[4] Ikerbasque
Calle de María Díaz de Haro 3, 48013 Bilbao, Basque Country – Spain
gpagnini@bcamath.org

Abstract: A novel approach to study the propagation of fronts with random motion is presented. This approach is based on the idea to consider the motion of the front, split into a drifting part and a fluctuating part; the front position is also split correspondingly. In particular, the drifting part can be related to existing methods for moving interfaces, for example, the Eulerian level set method and the Lagrangian discrete event system specification. The fluctuating part is the result of a comprehensive statistical description of the system which includes the random effects in agreement with the physical properties of the system. The resulting averaged process emerges to be governed by an evolution equation of the reaction-diffusion type. Hence, following the proposed approach, when fronts propagate with a random motion, models based on methods for moving interfaces and those based on reaction-diffusion equations can indeed be considered complementary and reconciled. This approach turns out to be useful to simulate random effects in wildland fire propagation as those due to turbulent heat convection and fire spotting phenomena.

Keywords: random front, wildland fire propagation, turbulence, fire spotting

MSC: 60K37, 62P12, 62P35, 82Dxx

1. Introduction

Modelling moving interfaces is an important issue in many research fields and in several real world applications. In many natural phenomena the front propagates into systems characterized by randomness and therefore the motion of the front gets a random character. Here a novel formulation for modelling random front motion is presented and its application to wildland fire propagation discussed.

Wildland fire propagation is a complex multi-scale, as well as a multi-physics and multi-discipline process, strongly influenced by the atmospheric wind. Wildland fire is fed by the fuel on the ground and displaced, beside meteorological and orographical factors, also by the hot air that pre-heats the fuel and aids the fire propagation. Heat transfer is turbulent due to the heat release in the Atmospheric Boundary Layer and the fire-induced flow. Moreover, fire generates firebrands which after landing on the ground act as new sources of fire. Both turbulence and jump-length of firebrands are random processes that affect the fireline propagation.

Fire propagation has been mainly modelled in the literature by using methods for simulating moving interfaces as the Eulerian level set method (LSM) [17], see e.g. [6, 7], or the Lagrangian discrete event system specification (DEVS) [4, 11] with the fire propagation solver ForeFire, see e.g. [3, 2], and reaction-diffusion type equations, see e.g. [1, 8].

These two approaches, namely that based on moving interface methods and that based on reaction-diffusion equations, are considered alternatives to each other because the solution of the reaction-diffusion equation is generally a continuous smooth function that has an exponential decay, and it is not zero in an infinite domain, while methods for simulating moving interfaces are associated to an indicator function that is 1 in the inner domain and 0 outside. However, when random processes (as for example hot air turbulent convection and fire spotting) are taken into account according to the proposed formulation, these two approaches can indeed be considered complementary and reconciled.

2. Random front model formulation

The proposed approach is based on the idea to consider the motion of the front split into a drifting part and a fluctuating part and the front position is split correspondingly. This splitting allows specific numerical and physical choices that can improve the algorithms and the models. In particular, the drifting part can be related to existing methods for moving interfaces, for example, the Eulerian LSM [17] or the Lagrangian DEVS [4, 11], and this permits the choice of the best method for any specific application. The fluctuating part is the result of a comprehensive statistical description of the system which includes the random effects in agreement with the physical properties of the system.

The resulting averaged process emerges to be governed by an evolution equation of the reaction-diffusion type. Hence, following the proposed approach, when fronts propagate with a random motion, models based on methods for moving interfaces and

those based on reaction-diffusion equations can indeed be considered complementary and reconciled.

Let Γ be a simple closed curve, or an ensemble of simple non-intersecting closed curves, representing a propagating interface in two dimensions, and let S be the domain of interest $S \subseteq R^2$. In the case of Γ being an ensemble of n curves, the ensemble of the n interfaces is considered to be an *interface*.

The subset of the domain S corresponding to the region Ω enclosed by Γ may be conveniently identified by an indicator function $I_\Omega : S \times [0, +\infty[\to \{0, 1\}$ defined as follows

$$
I_\Omega(\boldsymbol{x}, t) = \begin{cases} 1, & \boldsymbol{x} \in \Omega, \\ \\ 0, & \text{elsewhere.} \end{cases} \tag{1}
$$

In the case of a front line Γ made of more than one closed curve, the domain Ω is not simply connected, resulting in more than one sourrounded area evolving independently.

The indicator function I_Ω at time $t = 0$, i.e. $I_\Omega(\boldsymbol{x}, t = 0)$, describing the initial topology of the front, is indicated in the following as $I_{\Omega_0}(\boldsymbol{x}_0)$.

Let $\boldsymbol{X}^\omega(t, \overline{\boldsymbol{x}}_0) = \overline{\boldsymbol{x}}(t, \overline{\boldsymbol{x}}_0) + \eta^\omega$ be the ω-realization of a random trajectory driven by the random noise η. For every realization, the initial condition is stated to be $\boldsymbol{X}^\omega(0, \overline{\boldsymbol{x}}_0) = \overline{\boldsymbol{x}}_0$. Using the sifting property of δ-function, i.e. $g(\boldsymbol{x}) = \int g(\overline{\boldsymbol{x}}) \, \delta(\boldsymbol{x} - \overline{\boldsymbol{x}}) \, d\overline{\boldsymbol{x}}$, the evolution in time of the ω-realization of a random front contour $\gamma^\omega(\boldsymbol{x}, t)$ is given by

$$
\gamma^\omega(\boldsymbol{x}, t) = \int_S \gamma(\overline{\boldsymbol{x}}_0) \, \delta(\boldsymbol{x} - \boldsymbol{X}^\omega(t, \overline{\boldsymbol{x}}_0)) \, d\overline{\boldsymbol{x}}_0, \tag{2}
$$

which in terms of the random indicator $I_{\Omega^\omega}(\boldsymbol{x}, t)$ reads

$$
\begin{aligned}
I_{\Omega^\omega}(\boldsymbol{x}, t) &= \int_S I_{\Omega_0}(\overline{\boldsymbol{x}}_0) \, \delta(\boldsymbol{x} - \boldsymbol{X}^\omega(t, \overline{\boldsymbol{x}}_0)) \, d\overline{\boldsymbol{x}}_0 \\
&= \int_{\Omega_0} \delta(\boldsymbol{x} - \boldsymbol{X}^\omega(t, \overline{\boldsymbol{x}}_0)) \, d\overline{\boldsymbol{x}}_0 = \int_{\Omega(t)} \delta(\boldsymbol{x} - \boldsymbol{X}^\omega(t, \overline{\boldsymbol{x}})) \, d\overline{\boldsymbol{x}},
\end{aligned} \tag{3}
$$

where an incompressibility-like condition $\dfrac{d\overline{\boldsymbol{x}}_0}{d\overline{\boldsymbol{x}}} = 1$ is assumed.

Let $\varphi_e(\boldsymbol{x}, t) : S \times [0, +\infty[\to [0, 1]$ be an *effective indicator*. It may be defined as

$$
\begin{aligned}
\varphi_e(\boldsymbol{x}, t) = \langle I_{\Omega^\omega}(\boldsymbol{x}, t) \rangle &= \left\langle \int_{\Omega(t)} \delta(\boldsymbol{x} - \boldsymbol{X}^\omega(t, \overline{\boldsymbol{x}})) \, d\overline{\boldsymbol{x}} \right\rangle = \int_{\Omega(t)} \langle \delta(\boldsymbol{x} - \boldsymbol{X}^\omega(t, \overline{\boldsymbol{x}})) \rangle \, d\overline{\boldsymbol{x}} \\
&= \int_{\Omega(t)} f(\boldsymbol{x}; t | \overline{\boldsymbol{x}}) \, d\overline{\boldsymbol{x}} = \int_S I_\Omega(\overline{\boldsymbol{x}}, t) f(\boldsymbol{x}; t | \overline{\boldsymbol{x}}) \, d\overline{\boldsymbol{x}},
\end{aligned} \tag{4}
$$

where $\langle \cdot \rangle$ is the ensemble average and $f(\boldsymbol{x}; t|\overline{\boldsymbol{x}}) = \langle \delta(\boldsymbol{x} - \boldsymbol{X}^\omega(t, \overline{\boldsymbol{x}})) \rangle$ is the probability density function (PDF) of fluctuations of the perimeter around the contour $\Gamma(t)$.

Since the present approach is formulated to study the effects of an underlying diffusive process in front propagation, according to classical properties of diffusion, the resulting PDF $f(\boldsymbol{x}; t|\overline{\boldsymbol{x}})$ of the stochastic process $\boldsymbol{X}^\omega$ is considered to be unimodal and its mean and median are coincident. This means that $f(\boldsymbol{x}; t|\overline{\boldsymbol{x}})$ is a symmetric probability distribution which normalizes after integration both over $\boldsymbol{x}$ and $\overline{\boldsymbol{x}}$. Consequently, values of the effective indicator $\varphi_e(\boldsymbol{x}, t)$ range in the compact interval $[0, 1]$.

The front line $\Gamma(t)$ can be obtained by existing methods for moving interfaces, as for example the already mentioned LSM or DEVS. For a deterministic motion, it holds $f(\boldsymbol{x}; t|\overline{\boldsymbol{x}}) = \delta(\boldsymbol{x} - \overline{\boldsymbol{x}})$ and the result reduces to that of the chosen moving interface method, i.e. $I_\Omega(\boldsymbol{x}, t)$.

The evolution of the effective indicator $\varphi_e(\boldsymbol{x}, t)$ can be estimated by applying in (4) the Reynolds transport theorem [12]

$$\frac{\partial \varphi_e}{\partial t} = \int_{\Omega(t)} \frac{\partial f}{\partial t} \, d\overline{\boldsymbol{x}} + \int_{\Omega(t)} \nabla_{\overline{\boldsymbol{x}}} \cdot [\boldsymbol{V}(\overline{\boldsymbol{x}}, t) f(\boldsymbol{x}; t|\overline{\boldsymbol{x}})] \, d\overline{\boldsymbol{x}} \,. \tag{5}$$

Let $f(\boldsymbol{x}; t|\overline{\boldsymbol{x}})$ be the solution of the evolution equation,

$$\frac{\partial f}{\partial t} = \mathcal{E} f \,, \quad f(\boldsymbol{x}; 0|\overline{\boldsymbol{x}}_0) = \delta(\boldsymbol{x} - \overline{\boldsymbol{x}}_0) \,, \tag{6}$$

with $\mathcal{E} = \mathcal{E}(\boldsymbol{x})$ a generic evolution operator not acting on both $\overline{\boldsymbol{x}}$ and t, then equation (5) becomes the following reaction-diffusion type equation

$$\frac{\partial \varphi_e}{\partial t} = \mathcal{E} \varphi_e + \int_{\Omega(t)} \nabla_{\overline{\boldsymbol{x}}} \cdot [\boldsymbol{V}(\overline{\boldsymbol{x}}, t) f(\boldsymbol{x}; t|\overline{\boldsymbol{x}})] \, d\overline{\boldsymbol{x}} \,, \tag{7}$$

where $\boldsymbol{V}(\boldsymbol{x}, t)$ is the expansion velocity of the domain $\Omega(t)$ determined by $d\overline{\boldsymbol{x}}/dt = \boldsymbol{V}(\overline{\boldsymbol{x}}, t) = \mathcal{V}(\overline{\boldsymbol{x}}, t) \, \widehat{\boldsymbol{n}}$ and $\widehat{\boldsymbol{n}}$ is the normal to the front contour.

Finally, the front line is obtained by choosing an arbitrary threshold value φ_e^{th} which serves as the criterion to mark the inner region $\Omega_e(t) = \left\{ \boldsymbol{x} \in S | \varphi_e(\boldsymbol{x}, t) > \varphi_e^{th} \right\}$.

The above formulation has been considered for applications to diffusive media governed by fractional differential equations [9, 10]. In the following section, the application to wildland fire propagation is discussed.

3. Application to wildland fire propagation

In wildland fire propagation modelling, both the LSM and DEVS are adopted to simulate the evolution of the burning area, see e.g. [6, 7] and [3, 2], respectively. The

present approach can be used with both the methods to include random processes such as turbulence and fire spotting.

In particular, let $\boldsymbol{X}^\omega(t, \overline{\boldsymbol{x}}_0) = \overline{\boldsymbol{x}}(t, \overline{\boldsymbol{x}}_0) + \chi^\omega + \xi^\omega$ be the ω-realization of a random trajectory driven by the random noises χ and ξ corresponding to turbulence and fire spotting, respectively. For every realization, the initial condition is stated to be $\boldsymbol{X}^\omega(0, \overline{\boldsymbol{x}}_0) = \overline{\boldsymbol{x}}_0$. Average turbulent fluctuations are zero, i.e. $\langle \chi \rangle = 0$, and fire spotting is assumed to be independent of turbulence and to be a downwind phenomenon such that $\xi^\omega = \ell^\omega \, \widehat{\boldsymbol{n}}_U$, where ℓ is the landing distance from the main fireline such that $\langle \ell \rangle > 0$ and $\widehat{\boldsymbol{n}}_U$ is the mean wind direction.

The modelling of the random processes is handled by the PDF $f(\boldsymbol{x}; t|\overline{\boldsymbol{x}})$, accounting for the sum of the two independent random variables $(\overline{\boldsymbol{x}} + \chi)$ and ξ, representing turbulence and fire spotting respectively. This means that $f(\boldsymbol{x}; t|\overline{\boldsymbol{x}})$ is determined by the convolution between the PDF corresponding to $(\overline{\boldsymbol{x}} + \chi)$, hereinafter labeled as G, and the PDF corresponding to ξ, hereinafter labeled as q.

Since fire spotting is assumed to be an independent downwind phenomenon, the effect of fire spotting is accounted for only the leeward part of the fireline. Taking into account previous assumptions $f(\boldsymbol{x}; t|\overline{\boldsymbol{x}})$ results in

$$
f(\boldsymbol{x}; t|\overline{\boldsymbol{x}}) = \begin{cases} \displaystyle\int_0^\infty G(\boldsymbol{x} - \overline{\boldsymbol{x}} - \ell\widehat{\boldsymbol{n}}_U; t) \, q(\ell; t) \, d\ell, & \text{if} \quad \widehat{\boldsymbol{n}} \cdot \widehat{\boldsymbol{n}}_U \geq 0, \\[2mm] G(\boldsymbol{x} - \overline{\boldsymbol{x}}; t), & \text{otherwise}. \end{cases} \tag{8}
$$

Since the effective fireline contour $\varphi_e(\boldsymbol{x}, t)$ is a smooth function continuously ranging from 0 to 1, a criterion to mark burned points have to be stated. For example, points $\boldsymbol{x}$ such that $\varphi_e(\boldsymbol{x}, t) > \varphi_e^{th} = 0.5$ are marked as burned and the effective burned area emerges to be $\Omega_e(t) = \{\boldsymbol{x} \in S | \varphi_e(\boldsymbol{x}, t) > \varphi_e^{th} = 0.5\}$. However, beside this criterion, a further criterion associated to an ignition delay due to the pre-heating action of the hot air or to the landing of firebrands is introduced. Hence, in the proposed modelling approach, an unburned point $\boldsymbol{x}$ will be marked as burned when one of these two criteria is met.

This ignition delay, due to a certain *heating-before-burning mechanism*, can be depicted as an accumulation in time of heat [13, 14], i.e.

$$
\psi(\boldsymbol{x}, t) = \int_0^t \varphi_e(\boldsymbol{x}, s) \, \frac{ds}{\tau}, \tag{9}
$$

where $\psi(\boldsymbol{x}, 0) = 0$ corresponds to the unburned initial condition and τ is a characteristic ignition delay that can be understood as an electrical resistance. Since the fuel can burn because of two independent pathways, i.e. hot-air heating and firebrand

landing, the resistance analogy suggests that τ can be approximatively computed as resistances acting in parallel, i.e.

$$\frac{1}{\tau} = \frac{1}{\tau_h} + \frac{1}{\tau_f} = \frac{\tau_f + \tau_h}{\tau_h \tau_f} \,, \tag{10}$$

where τ_h and τ_f are the ignition delays due to hot air and firebrands, respectively.

The amount of heat is proportional to the increasing of the fuel temperature $T(\boldsymbol{x}, t)$, then

$$\psi(\boldsymbol{x}, t) \propto \frac{T(\boldsymbol{x}, t) - T(\boldsymbol{x}, 0)}{T_{ign} - T(\boldsymbol{x}, 0)} \,, \quad T(\boldsymbol{x}, t) \leq T_{ign} \,, \tag{11}$$

where T_{ign} is the ignition temperature.

Finally, when $\psi(\boldsymbol{x}, t) = 1$ the ignition temperature is assumed to be reached, so that a new ignition occurs in $(\boldsymbol{x}, t)$ and, with reference to (4), the modelled fire goes on by setting $I_\Omega(\boldsymbol{x}, t) = 1$. Then, as a consequence of the heating-before-burning mechanism described in (9), the domain $\Omega(t)$ is established as $\Omega(t) = \{\boldsymbol{x} \in S | I_\Omega(\boldsymbol{x}, t) = 1\}$ which is hard to be analytically evaluated but numerically computed only. The expansion velocity of the domain $\Omega(t)$ in the normal direction is stated by means of the prescription of the so-called Rate Of Spread (ROS).

4. Numerical simulations

To estimate the performance of the LSM based model and DEVS based model coupled with the random processes a series of simulation experiments are conducted. For LSM, a formulation developed in References [7, 6] is followed, while for DEVS, ForeFire fire simulator [3] is used. Both these models have a different formulation to incorporate the nature of vegetation and slope hence, it is tried to parametrise both models in an identical setup.

In the present study, for brevity no particular type of vegetation is defined and simulations are carried out with a pre-defined value of ROS. It is assumed that the ROS remains constant for a particular terrain. It is emphasised that these are simplified and idealised test cases and no attempt is made to choose the parameters for a realistic setup. The present scope of this work is to provide a first look into the investigation of comparing LSM and DEVS based fire simulations with random processes.

A flat area of hypothetical homogeneous vegetation spread over a domain size of $5000\,\mathrm{m} \times 5000\,\mathrm{m}$ is selected for simulations. Different values of the ROS are utilised for different test cases. The ROS is assumed to be $0.05\,\mathrm{ms}^{-1}$ in no wind conditions while, in the presence of wind, it is estimated by the 3% ROS model [2]:

$$ROS = 0.03\,\boldsymbol{U} \cdot \widehat{\boldsymbol{n}} \,, \tag{12}$$

where, U is the mean wind velocity. Since, 3% ROS considers the propagation only towards the mean wind direction, in order to study the evolution of the fireline towards the flank and rear the following ROS is also considered [6]:

$$ROS(U,\theta) = \begin{cases} \varepsilon_o + a\sqrt{U}\cos^n\theta, & \text{if } |\theta| \leq \frac{\pi}{2}, \\ \varepsilon_o(\alpha + (1-\alpha)|\sin\theta|), & \text{if } |\theta| > \frac{\pi}{2}, \end{cases} \tag{13}$$

where, ε_o is the flank velocity and $(\alpha\varepsilon_o)$ is the rear velocity with $\alpha \in [0,1]$, and θ is defined as the angle between the normal to the front $\widehat{\boldsymbol{n}}$ and the mean wind direction $\widehat{\boldsymbol{n}}_U$. For the present setup, we assume the values $\alpha = 0.8$, $n = 3$, $a = 0.5\,\mathrm{m}^{1/2}\mathrm{s}^{-1/2}$, $\varepsilon_o = 0.2\,\mathrm{ms}^{-1}$.

In LSM, the domain is discretised with a Cartesian grid of 20 m in both x and y directions, while for DEVS the resolution of the simulation is defined in the terms of quantum distance Δq and perimeter resolution Δc [3]. The quantum distance Δq is defined as the maximum allowable distance to be covered by a particle at each advance, while a measure of Δc is used to decompose/regenerate/coalesce two particles on propagation. The choice of Δq and Δc is *dependent on the type of problem*, and in the present study two sets of values are used. The simulation is performed with $\Delta q = 4\,\mathrm{m}$, $\Delta c = 18\,\mathrm{m}$ for zero wind; and $\Delta q = 0.3\,\mathrm{m}$, $\Delta c = 8\,\mathrm{m}$ in the presence of wind. To avoid instability in the presence of wind, Δq is chosen to be of a much higher resolution than the wind data (20 m in this setup). The time is advanced according to the events in ForeFire, and the simulation can move ahead according to a user defined time. To facilitate a comparison between the two models, the simulation in DEVS model is advanced by the time step computed according to the Courant–Friedrichs–Lewy (CFL) criteria in LSM.

The mean wind, wherever used, is assumed to be constant in magnitude and direction. The turbulence is modelled according to a bi-variate Gaussian PDF

$$G(\boldsymbol{x} - \overline{\boldsymbol{x}}; t) = \frac{1}{2\pi\sigma^2(t)} \exp\left\{ -\frac{(x - \overline{x})^2 + (y - \overline{y})^2}{2\,\sigma^2(t)} \right\}, \tag{14}$$

where σ^2 is the particle displacement variance related to the turbulent diffusion coefficient $\mathcal{D}$, such that $\langle(x - \overline{x})^2\rangle = \langle(y - \overline{y})^2\rangle = \sigma^2(t) = 2\mathcal{D}t$. In the present model, the whole effect of the turbulent processes over different scales is assumed to be parametrised by the turbulent diffusion coefficient only.

The phenomenon of fire spotting is included according to the discussion provided in References [16] and [5]. In Reference [16] it is shown that the firebrand distribution followes a bimodal distribution but only the contribution of the firebrands with short landing distance is significant because the ones with long-distance landing reach the ground in charred oxidation state. According to this, the distribution of the firebrands follows a log-normal distribution [16]

$$q(\ell; t) = \frac{1}{\sqrt{2\pi}\,s(t)\ell} \exp\left\{ -\frac{(\ln\ell - \mu(t))^2}{2\,s^2(t)} \right\}, \tag{15}$$

where, $\mu(t) = \langle \ln \ell \rangle$ and $s(t) = \langle (\ln \ell - \mu(t))^2 \rangle$ are the mean and the standard deviation of $\ln \ell$ respectively. They are stated to be [15]

$$\mu = 1.32 I_f^{0.26} U^{0.11} - 0.02 \tag{16}$$
$$s = 4.95 I_f^{-0.01} U^{-0.02} - 3.48 \tag{17}$$

where U is the magnitude of the mean wind and $I_f = I + I_t$ represents fire intensity I enriched by the tree torching intensity I_t. The turbulent diffusion coefficient $\mathcal{D}$ and ignition delay τ are also assumed to be constant throughout the simulations. The value of $\mathcal{D}$ is assumed to be $0.15\,\mathrm{m^2 s^{-1}}$ and the ignition delay for hot air and firebrand is fixed at $600\,\mathrm{s}$ and $60\,\mathrm{s}$ respectively. The initial fire intensity is assumed to be $10\,000\,\mathrm{kWm^{-1}}$ and the tree torching intensity is fixed at $0.015\,\mathrm{kWm^{-1}}$.

A series of idealised simulation tests are made to investigate the behaviour of the two models with identical initial conditions. Different simulations are performed both in the presence and the absence of wind by neglecting and considering the random processes. The first case evaluates an isotropic growth of the fireline for zero wind in both the models by neglecting all the random processes. In the second test, the spread of fireline for different ROS in different directions is studied. The third test discusses the propagation of the fireline with wind when the ROS is defined according to the 3% formula (12) and to formula (13). The random processes are neglected for the first three test cases. The fourth test presents the evolution of fireline when turbulent processes are included both in the presence and absence of wind. The last test evaluates the performance when fire spotting also included along with turbulence. Firebreak lines are also introduced in the last two tests to highlight the propagation of the fireline while encountering areas of null fuel. It should be noted that for brevity fire spotting is assumed to be an independent downwind phenomenon. Hence, the effect of fire spotting is accounted for only the leeward part of the fireline. Also, to simplify the simulation, the region across and behind the centre of the initial fireline is demarcated as the leeward side and the windward side respectively.

5. Discussion

Figure 1 presents the evolution of the fireline for a circular initial condition of radius $300\,\mathrm{m}$ for both LSM based model and DEVS based model. In the absence of the wind, the initial circular fireline is transported into a isotropic growth, and the circular contours correspond to $40\,\mathrm{min}$ isochronous fronts. It can very well appreciated that with the same value of ROS and initial conditions, the two different tracking schemes provide an identical evolution of the fireline. Modelling real situations of fire involves presence of zones without fuel, where the ROS is zero. In case of firebreak zones, pure LSM and DEVS are inherently unable to simulate the realistic situations of fire overcoming a fire break. Figure 2 shows that the fireline fails to propagate across the firebreak when no random processes are included. The
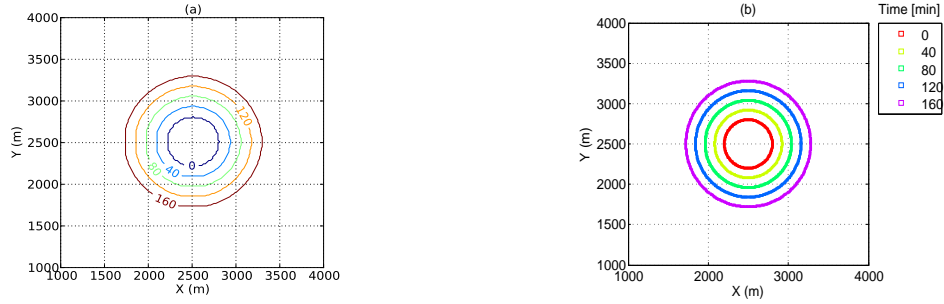
Figure 1: Evolution in time of the fireline contour without random processes and zero wind for a) LSM and b) ForeFire. The initial fireline is a circle of radius 300 m.
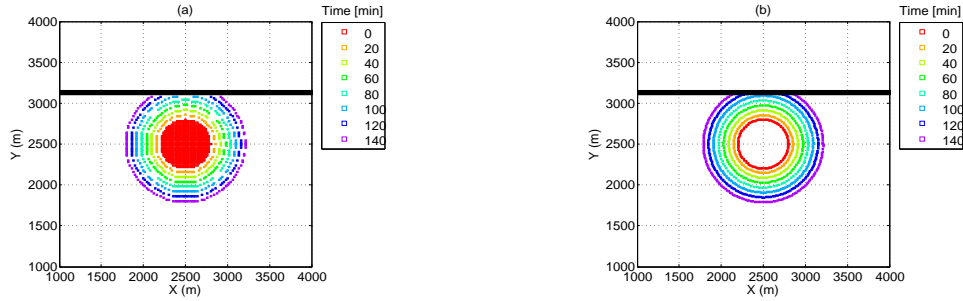

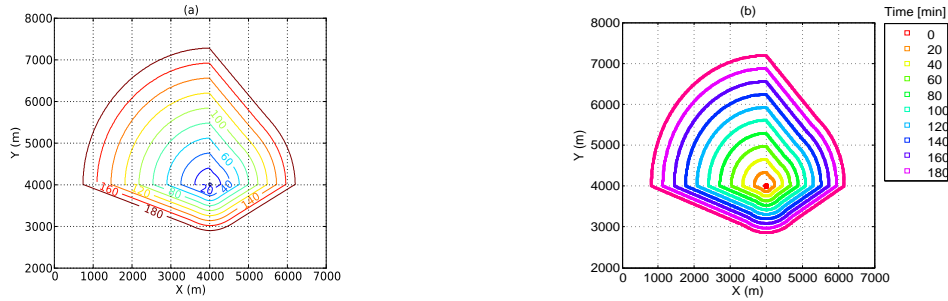Figure 2: Same as Figure 1, but in the presence of a firebreak zone (60 m wide).

Figure 3: Same as Figure 1, but with a non-homogeneous ROS. The ROS is $0.3\,\mathrm{ms}^{-1}$, $0.2\,\mathrm{ms}^{-1}$, $0.1\,\mathrm{ms}^{-1}$ in upper-left, upper right and bottom quadrants respectively.

evolution is shown only upto 140 min, but an extended run upto 250 min indicates the limitation of the models to simulate the fire jump across the break zone.

Figure 3 presents the growth of an initial spot fire but with a non-homogenous ROS in absence of any wind. The different values of the ROS can be attributed to different fuel types. The fireline propagates with different speed in the three directions. In the absence of wind, the two tracking methods show an identical behaviour in simulating situations with constant ROS. This paves way for a comparison of situations with higher variability and complexity.
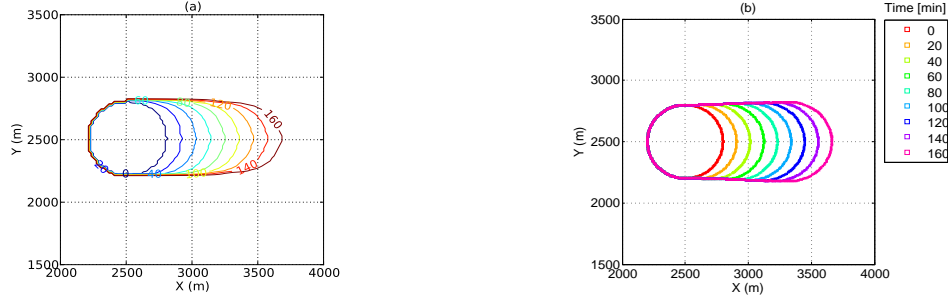
93

Figure 4: Same as Figure 1, but when the mean wind velocity is $3\,\mathrm{ms}^{-1}$ in the positive x-direction.
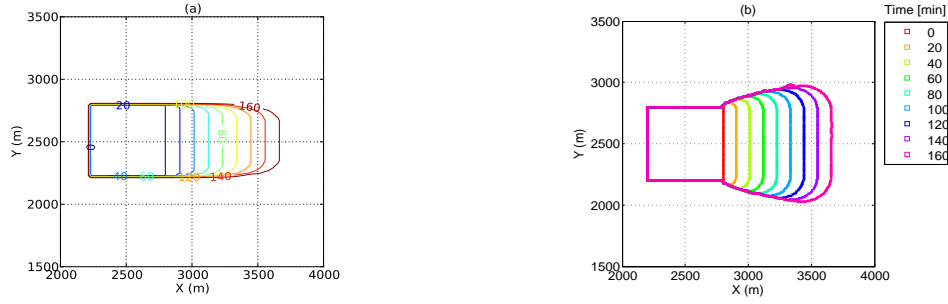

Figure 5: Same as Figure 4, but when the initial profile is square with side $600\,\mathrm{m}$.

Figure 4 shows the evolution of the firefront with a circular initial profile (with radius $300\,\mathrm{m}$) in case of a light wind of $3\,\mathrm{ms}^{-1}$ directed in the positive x direction. The isochronous fronts are plotted at every $20\,\mathrm{min}$ and follow an oval shape for both the models. The fire contours in DEVS based model diverge slightly from the mean wind field and an increasing flanking fire develops over time. This divergence in the evolution of firefront occurs due to differences in the computation of the normal for both the models. The computation of normal for an active fire point in DEVS model is approximated as the measure of the bisector of the angle between the point and its left and right neighbours. This fact can be very well appreciated when an initial square profile is considered.

Figure 5 shows the evolution of the fire spread with square initial profile of side $600\,\mathrm{m}$. Under the effect of the constant zonal wind, the evolution in LSM strictly follows the initial square shape, while in ForeFire the initial angular points are transported to provide a flanking spread. The 3% ROS does not model the rear and back fire but DEVS generates spurious flanking fire that gives a realistic behaviour to the fire spread even if due to the approximate construction of the front normal. The differences in the evolution of flank fireline are also studied by introducing different ROS for the head, flank and rear directions according to (13). Here θ is defined as the angle between the normal to the front and the mean wind direction. Since the normal computation in DEVS approach is approximate, two
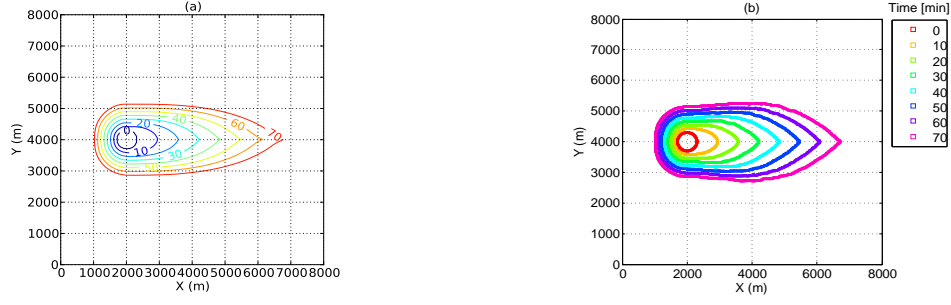
Figure 6: Evolution in time of the fireline contour without random processes with ROS given by formula (13) where θ is the angle between the outward normal in a contour point and the mean wind direction for a) LSM and b) ForeFire. The mean wind velocity is $3\,\text{ms}^{-1}$ in the positive x-direction.
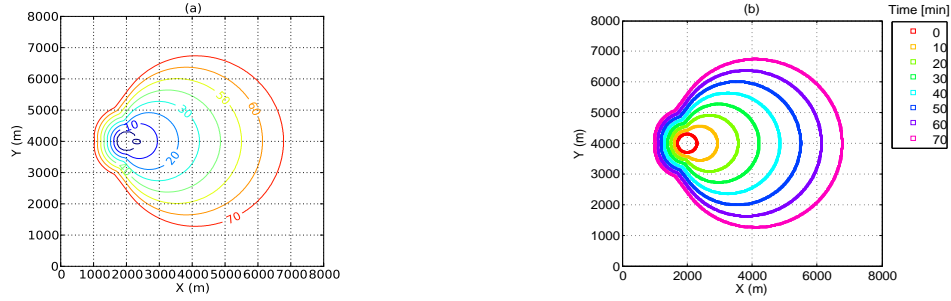

Figure 7: Same as Figure 6, but where θ is the angle between the line joining a contour point and the centre of the initial burned area.

separate tests are performed to evaluate effect of the normal on the spread: firstly when θ is computed according to the definition, and secondly, to ensure identical angle for both methods, when θ is assumed to be the angle between the line joining a contour point and the centre of the initial burned area. Figure 6 shows that when θ is computed in accordance to the definition, the simulations for head and rear fires are identical, but spurious flanks are observed for DEVS based model. On the other hand, it is evident from Figure 7 that identical values of θ shows an identical propagation of the fireline in all directions.

As shown above, in case of firebreak zones pure LSM and ForeFire are inherently unable to simulate the realistic situations of fire overcoming a fire break. But Figure 8 shows that with the introduction of turbulence the models can simulate the effect of hot air to overcome firebreak zone. The value of turbulent diffusion coefficient is assumed to be $0.15\,\text{m}^2\text{s}^{-1}$. The evolution of the fireline is almost similar for both the models, though a slight underestimation is visible in ForeFire with respect to the LSM based model. Stronger turbulence causes a more rapid propagation of the fireline and an earlier ignition across the firebreak zone. A detailed analysis of the effect of varying turbulence over *long-term propagation* with the LSM can be found in [13, 14].
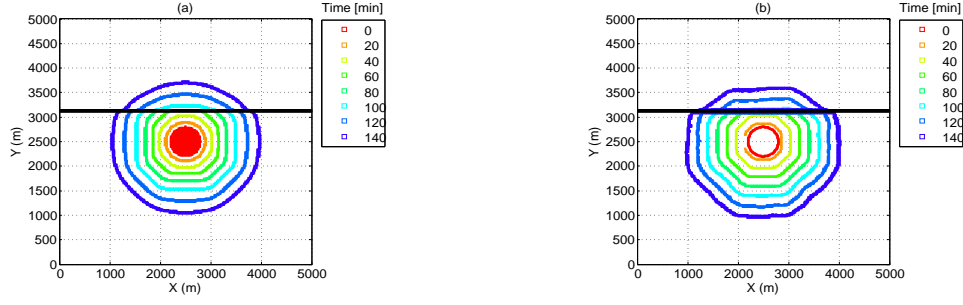
Figure 8: Evolution in time of the fireline contour with turbulence in zero wind for a) LSM and b) ForeFire. The initial fireline is a circle of radius $300\,\mathrm{m}$. The turbulent diffusion coefficient is $0.15\,\mathrm{m^2s^{-1}}$.
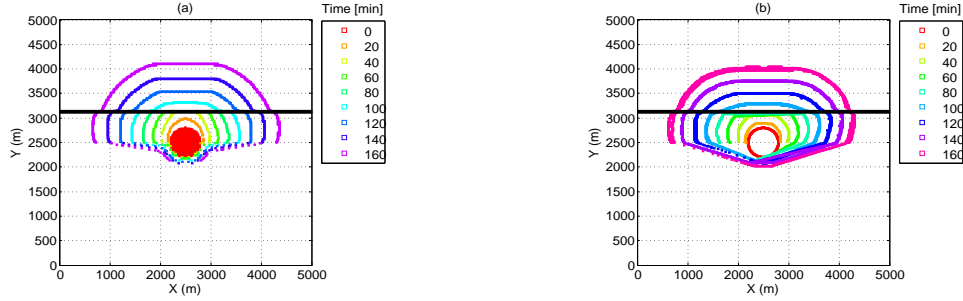

Figure 9: Same as Figure 8, but when the mean wind velocity is $3\,\mathrm{ms^{-1}}$ in positive y-direction.

Figure 9 presents the effect of inclusion of turbulence with a non-zero wind profile and 3%-wind ROS. The effect of turbulence is most pronounced in the direction of the mean wind and it clearly shows that randomisation of the fireline permits the fire to overcome the obstacle without fuel along with an increased growth in the flank-fire, back fire and head fire. Both models show almost similar characteristics in modelling the spread of fire, though the flank fire has a slightly larger spread in ForeFire. This is due to the fact the particle transportation in the direction of the front normal is computed with an approximated method.

Another aspect contributing towards the increase in the fire spread and allowing new fire ignitions across obstacles due to fire spotting is presented in Figure 10. With inclusion of fire spotting along with turbulence, the evolution of the fire front is faster in comparison to the effect of turbulence alone as seen in Figure 9. The region across the fire break has a quick ignition pertaining to the embers flowing and landing with the effect of wind. It should be noted that within the considered parametrisation (15) the phenomenon of fire spotting can only be observed in the presence of the wind. The flank fire and the head fire are also well simulated in both the models, and again a larger spread out the flanking fires is observed for DEVS. Fire spotting along with turbulence has a remarkable effect on enhancing the fireline and igniting secondary fires across the fire break zones.
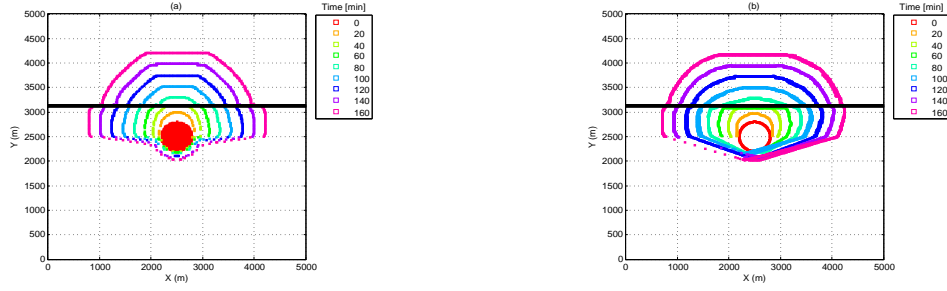
96

Figure 10: Same as Figure 9, but when phenomenon of fire-spotting is also included.

6. Conclusions

This paper describes an approach to model the effects of the random processes in the propagation of the wildland fires. The propagation of the fire can be split into a drifting part and a fluctuating part. The fluctuating part is generated by a comprehensive statistical description of the system and includes the effects of random processes in agreement with the physical properties of the system.

The drifting part is modelled in terms of a deterministic position determined by Eulerian LSM or Lagrangian DEVS with a certain ROS, and the fluctuating part according to the PDF of the random displacement of points marked as active burning points. Numerical simulations show that this formulation emerges to be suitable for both LSM and DEVS based models to manage the real world situations related to random character of fire e.g., increase in ROS due to pre-heating of the fuel by hot air and vertical lofting and transporting of firebrands and fire overcoming no fuel zones. DEVS computes an approximated outward normal of the fire perimeter that generates differences with the LSM. Such differences result in spurious flanking fires, which however provide a more realistic fire contour. The two models perform in agreement with each other and can be complementary to each other for simple situations, but for increasing complexity the introduction of random processes amplifies differences between DEVS and LSM which are mainly due to the approximate computation of normal.

Acknowledgements

References

[1] Asensio, M. I. and Ferragut, L.: On a wildland fire model with radiation. Int. J. Numer. Meth. Engng. **54** (2002), 137–157.

[2] Filippi, J. B., Mallet, V., and Nader, B.: Evaluation of forest fire models on a large observation database. Nat. Hazards Earth Syst. Sci. **14** (2014), 3077–3091.

[3] Filippi, J. B., Morandini, F., Balbi, J. H., and Hill, D.: Discrete event front tracking simulator of a physical fire spread model. Simulation **86** (2010), 629–646.

[4] Karimabadi, H., Driscoll, J., Omelchenko, Y. A., and Omidi, N.: A new asynchronous methodology for modeling of physical systems: breaking the curse of Courant condition. J. Comp. Phys. **205** (2005), 755–775.

[5] Kortas, S., Mindykowski, P., Consalvi, J. L., Mhiri, H., and Porterie, B.: Experimental validation of a numerical model for the transport of firebrands. Fire Safety J. **44** (2009), 1095–1102.

[6] Mallet, V., Keyes, D. E., and Fendell, F. E.: Modeling wildland fire propagation with level set methods. Comput. Math. Appl. **57** (2009), 1089–1101.

[7] Mandel, J., Beezley, J. D., and Kochanski, A. K.: Coupled atmosphere-wildland fire modeling with WRF 3.3 and SFIRE 2011. Geosci. Model. Dev. **4** (2011), 591–610.

[8] Mandel, J. et al.: A wildland fire model with data assimilation. Math. Comput. Simulat. **79** (2008), 584–606.

[9] Mentrelli, A. and Pagnini, G.: Random front propagation in fractional diffusive systems. Communications in Applied and Industrial Mathematics (2014). http://dx.doi.org/10.1685/journal.caim.504.

[10] Mentrelli, A. and Pagnini, G.: Front propagation in anomalous diffusive media governed by time-fractional diffusion. J. Comp. Phys. **293** (2015), 427–441.

[11] Omelchenko, Y. A. and Karimabadi, H.: HYPERS: A unidimensional asynchronous framework for multiscale hybrid simulations. J. Comp. Phys. **231** (2012), 1766–1780.

[12] Pagnini, G. and Bonomi, E.: Lagrangian formulation of turbulent premixed combustion. Phys. Rev. Lett. **107** (2011), 044 503.

[13] Pagnini, G. and Massidda, L.: The randomized level-set method to model turbulence effects in wildland fire propagation. In: D. Spano, V. Bacciu, M. Salis, and C. Sirca (Eds.), *Modelling Fire Behaviour and Risk. Proceedings of the International Conference on Fire Behaviour and Risk. ICFBR 2011, Alghero, Italy, October 4–6, 2011*, 126–131, 2012. ISBN 978-88-904409-7-7.

[14] Pagnini, G. and Massidda, L.: Modelling turbulence effects in wildland fire propagation by the randomized level-set method. Tech. Rep. 2012/PM12a, CRS4, 2012. Revised version August 2014, arXiv:1408.6129.

[15] Perryman, H. A., Dugaw, C. J., Varner, J. M., and Johnson, D. L.: A cellular automata model to link surface fires to firebrand lift-off and dispersal. Int. J. Wildland Fire **22** (2013), 428–439.

[16] Sardoy, N., Consalvi, J. L., Kaiss, A., Fernandez-Pello, A. C., and Porterie, B.: Numerical study of ground-level distribution of firebrands generated by line fires. Combust. Flame **154** (2008), 478–488.

[17] Sethian, J. A. and Smereka, P.: Level set methods for fluid interfaces. Ann. Rev. Fluid Mech. **35** (2003), 341–372.